Circularly Polarized Jute Textile Antenna for Wi-MAX, WLAN and ISM Band Sensing Applications

Ram Sandeep D. [1], Prabakaran N. [1], Madhav Boddapati T. P. [1], and Narayana K. L. [2]

[1] Department of ECE, KLEF, Guntur, 522502, India
askram91@gmail.com, prabakaran@kluniversity.in, btpmadhav@kluniversity.in

[2] Department of Mechanical Engineering, Guntur,522502, India
drkln@kluniversity.in

Abstract **─** This study exhibits a circularly polarized (CP) conformal antenna actualized by using a jute textile as a substrate. Its sensing 3.5, 4.9, and 5.8 GHz in the Wi-MAX, WLAN, and ISM radio bands. The topology of the proposed antenna has relied on a curvature structure as the prime radiating element, and ground structure whirled in contradictive arrangement to the patch. Conductivity was materialized by applying copper paint through the traditional painting approach, i.e., brush painting. This fabrication method allows attaining the conformability with minimized size, lightweight, and low sensitivity to the environment without weakening the radiating performance. These attributes allowed the jute textile antenna appropriately for the incorporation in wearable devices for body-driven applications. The electromagnetic properties of the projected jute textile antenna accomplished in simulations were confirmed through the measurement of the antenna in an anechoic chamber. The CP jute textile antenna shows a peak gain of 4.93, 8.86, and 10.07dBi at 3.5, 4.9, and 5.8 GHz (WiMAX, WLAN, and ISM).

Index Terms **─** Circular polarization, copper paint, ISM band, WiMAX, WLAN.

I. INTRODUCTION

Over the most recent couple of years, the implementation of wearable antennas for body-driven communication has drawn attention from engineers and researchers because of its increasing demand in the field of military and civil applications [1]. Traditional available rigid antennas are found difficult in mounting on the human body and causes discomfort owing to its inability to bend and move in different directions. The utilization of fabric materials as the substrate for micro-wave elements and structures seems to remain a desirable feature that ensures immense lead in the actualization of the wearable antennas for wireless communications. This developing attention has promoted the realization of numerous antenna topologies, together with printed dipoles [2], and patch antennas [3] with the underlying principle of decreasing its size and increasing its efficiency. Also, textile antennas (textenna) utilizing the snap-on push button were lately proposed [4].

Because of the recurrent movement of the human body, it gets hard to stabilize polarization align of the transceiver nodes for better power reception. Therefore, the circular polarization (CPn) feature aptly substitutes the need for continual aligning of the two nodes for maximum power reception. It also has many added advantages like exhibits resistance to signal degradation reported out of climatic changes, provides a highly reliable communication link, and overcome multipath effects [5-7]. In [8], the authors proposed a CP Jia-shaped antenna; the CPn is achieved by optimizing the feed position. A dual-band annually slot antenna for dual sense CPn was presented [9]. In [10], a 3-d CP helix antenna was reported on the FR-4 substrate with wide 3db beamwidth. A reconfigurable polarization antenna was proposed for WLAN applications; two-pin diodes are used to achieve polarization diversity [11]. In [12], the authors presented both frequency and polarization reconfigurable antenna duly operating in five different states by using five-pin diodes. Most of these works are developed on rigid substrates, which are found not fit for on-body communication applications.

This study exhibits a novel CP semicircular shaped antenna inspired by a very famous Tai-Chi symbol accomplished with textile materials. Many parameters are needed to consider while designing a textenna since wearable antennas work in proximity to the human body, in addition to antenna properties such as form factor, polarization, bandwidth, and weight should also be deliberately considered. It is imperative to take note that there are very few textennas structures that can fulfill these prerequisites all the while.

The objectives of the present work were to:

(i) Use textile materials as substrates which are either effectively utilized in the textile manufacturing plant, or readily available in the native market.

Submitted On: January 21, 2020
Accepted On: October 20, 2020

https://doi.org/10.47037/2020.ACES.J.351206

1054-4887 © ACES

(ii) Carry out a fabrication procedure that is basic and appropriate enough to be helpful for industry line production.
(iii) Designing it as compact and low-profile to fit on the clothing of the wearer, hence its presence outwardly unnoticeable and doesn't cause discomfort to the wearer.
(iv) Make it practical for on-body communication with CP.

II. MATERIAL AND ANTENNA DESIGN

In respect of the substrates incorporated for actualization of the textenna, in this present writeup, various textiles have been utilized. A few such fabric materials are considered to be as cotton and silk. Based on the magnetic, electrical properties of the material and the access feasibility, textile selection has been considered. While making use of the textile substrates, it should primarily be adaptable and non-mutilative; besides, it must exhibit proper mechanical features (for example, homogeneity in thickness). Also, its humidity recapture ought to remain <7%, with the end goal that the textenna attributes stay steady under diverse relative moisture circumstances.

In the present work, treated jute fibers with a thickness of 1.5 mm were chosen, due to its flexibility, low moisture retention, and lightness. Moreover, the conductive copper paint sits well on its surface, and it is shock-absorbent too. Comparative analysis of various antenna models on different substrates are presented in Table 1.

Table 1: Comparative study of the proposed textile antenna with the recent works

Reference and Substrate	**Dimensions (mm^3)**	**Frequency (GHz) & Applications**	**Gain (dBi) & Circular Polarization (Yes or No)**
[13] Textile	57×32.1×3.6	2.45 (ISM)	3.39 (no)
[14] FR4	50×50 ×1.6	2.3 (WI-MAX)	2.7 (no)
[15] FR4	100×90×3.3	2.42 (WLAN)	5 (no)
[16] Textile	140×80×5	2.45 (ISM)	6.8 (no)
This work (Jute textenna)	20×16 ×1.5	3.5 (WI-MAX), 4.9 (WLAN), 5.8(ISM)	4.93, 8.86, 10.07 (yes)

The proposed antenna geometry is shown in Fig. 1, and detailed dimensions are provided in Table 2. The design and simulations of proposed textenna are carried out by Ansys HFSS 19.0 software. Conductive copper paint is brush painted on cotton, silk, and jute with a thickness of 0.6, 0.4, and 1.5 mm, respectively.

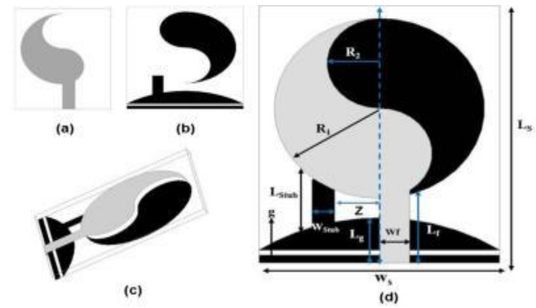

Fig. 1. Proposed antenna: (a) front plane, (b) ground plane, (c) adjacent view, and (d) geometry of CP jute textenna.

Table 2: The proposed antenna geometry in detail (mm)

L_s	W_s	W_f	L_f
20	16	2	5
h	g	L_{stub}	W_{stub}
1.5	0.5	2.5	1.5
R1	R2	L_g	Z
7	3.5	2.5	2.5

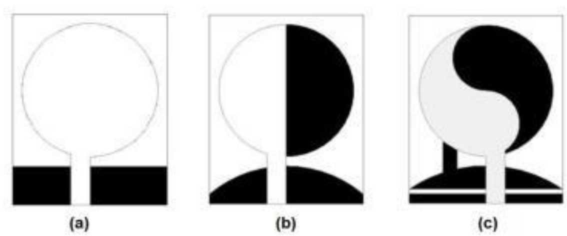

Fig. 2. Iteration wise evolution of the proposed textenna: (a) first iteration, (b) second iteration, and (c) third iteration.

The proposed antenna is developed from a circular structure, and its evolution steps are illustrated in Fig. 2. As shown in Fig. 2 (a) in first iteration, a simple circular patch with a 7mm radius (R_1) was taken in the radiating side, and a similar circular like entity on a rectangle was placed in the ground plane. Figure 4 illustrates the resonating frequencies concerning iteration steps, for the first iteration, it is resonated at dual-band with a span of 3.65 to 5.4 GHz and 6.4 to 9.4 GHz. The radius of the circle (R_1) plays a crucial role in determining the resonating frequency. The radius value R_1 is parametrized from 6-8 mm along with the ground structure that contains a similar circle. Figure 3 illustrates the frequency response concerning the change of radius from 6-8 mm. The radius of the circular patch structure [17] is given by equation (1):

$$a = \frac{F}{\left\{1+\frac{2h}{\pi \epsilon_r F}\left[\ln\left(\frac{\pi F}{2h}\right)+1.7726\right]\right\}^{\frac{1}{2}}}, \quad (1)$$

$$F = \frac{8.791\times 10^9}{f_r\sqrt{\epsilon_r}}. \quad (2)$$

By considering the fringing effects. The effective radius of the patch is given by:

$$a_e = a\left\{1+\frac{2h}{\pi \epsilon_r a}\left[\ln\left(\frac{\pi a}{2h}\right)+1.7726\right]\right\}^{\frac{1}{2}}. \quad (3)$$

Where h is the height of the substrate, ε_r is the dielectric constant, f_r is the resonant frequency.

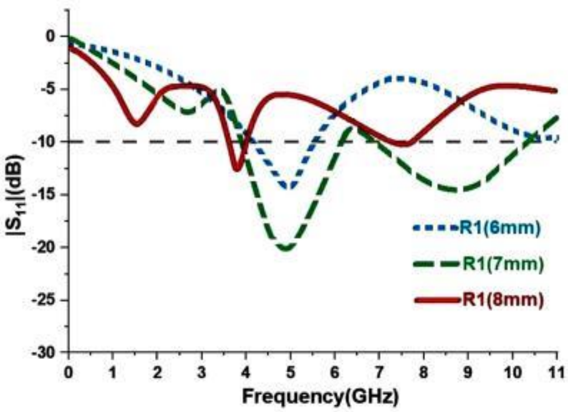

Fig. 3. Frequency response to the parametric analysis of radius R_1 (6-8 mm).

For a radius of 6 mm, the antenna resonated at 4.9 GHz with a return loss of -14 dB. For a radius of 8 mm, it resonated at 3.5 with a return loss of -13 dB. From the above parametric analysis, the circular patch with a 7 mm radius resonated better with dual-band than 6 and 8mm. So, a radius of 7 mm was considered in the patch and ground structures. The first iteration model did not operate with a CPn in any of the operating bands.

In the second iteration, as shown in Fig. 2 (b), the circular patch and ground structures are divided into two equal halves that are arranged in an inverse direction in patch and ground, respectively. The ground plane rectangular structure is changed as a semi-elliptical structure. The wide bands in the first iteration are now converted as a narrow band and resonating at 3.15, 4.95, and 6.40 GHz consecutively. As illustrated in Fig. 5, the values of the axial ratios (ARs) of this model are not under the 3db range, so it does not operate with a CPn. In the third iteration, as shown in Fig. 2 (c), the antenna patch comprises a half with radius R_1 (7 mm) in which two crescents with radius R_2 (R_2=R_1/2) are evacuated and integrated on top and bottom of the half-circle (R_1), separately. A stereotype of alterations are adapted in the ground plane, contrarily.

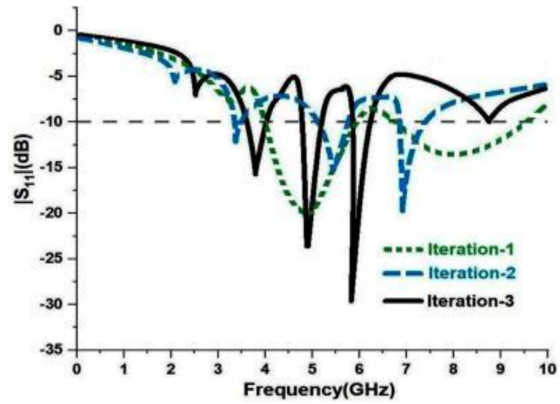

Fig. 4. Iteration wise results of the reflection coefficient.

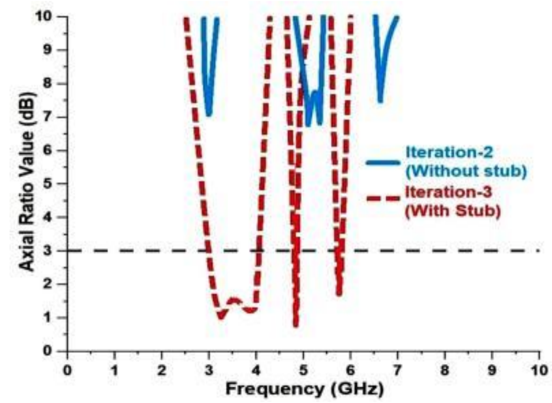

Fig. 5. Iteration wise results of the axial ratios (ARs).

The antenna ground was built on a rectangular structure over which a semi-elliptical structure with a stub was placed. The essential parameters for attaining CPn and impedance matching at the resonating frequencies are the L_{stub} (stub length) and the Z (the distance from the symmetric axis to the stub). The effect of the stub on CPn is illustrated in Fig. 5. For achieving a decent impedance matching between the patch of the antenna and 50 Ω port, the asymmetric microstrip line is used, where L_f is the length, and W_f is the width of the feed line. As illustrated in Fig. 4, this final model resonated at 3.5, 4.9, and 5.8 GHz successively with a CPn feature.

In this study, to realize the conductive parts of the antenna, the copper paint was utilized, which can be brush-painted. Using this unique approach, the proposed antenna design was brush painted on cotton, silk, and jute substrate. Figure 6 shows the 10x optical zoom images of cotton, silk, and jute textiles, taken by a digital single-lens reflector camera to show the surface structural differences and fiber intervention. Photographs of the cotton, silk, and jute textile antenna prototypes are shown in Fig. 7.

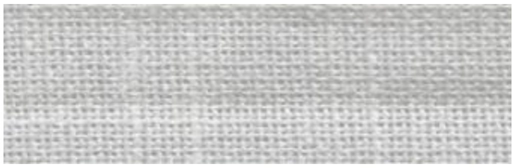
(a)

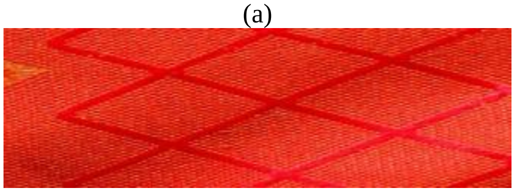
(b)


(c)

Fig. 6. Photographs of textiles in 10x optical zoom: (a) cotton, (b) silk, and (c) jute.

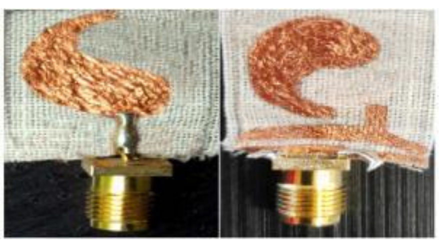
(a)

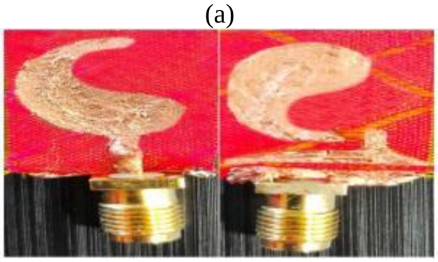
(b)

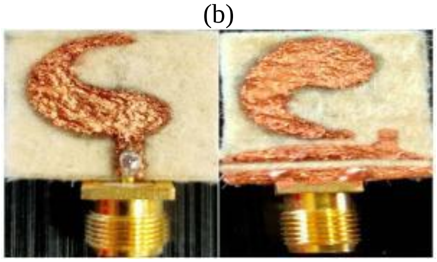
(c)

Fig. 7. Photos of :(a) cotton fabricated model front plane, and ground plane, (b) silk fabricated model front plane and ground plane, and (c) CP jute textile fabricated model front plane, and the ground plane.

III. RESULT ANALYSIS

Performance of the antennas were studied in free space, and all the simulated models are experimentally verified to evaluate the performance. Figure 8 (a) shows the simulated and measured reflection coefficient of the CP jute fabricated model, which resonates at 3.5, 4.9, and 5.8 GHz. The specifications of WiMAX, WLAN, and ISM are satisfied (return loss >10dB). The same design was fabricated on cotton and silk textiles to examine the responses concerning the change of textiles. They resonated at 4.6 GHz (Fig. 8 (b)) and 5.15, 9.35 GHz (Fig. 8 (c)).

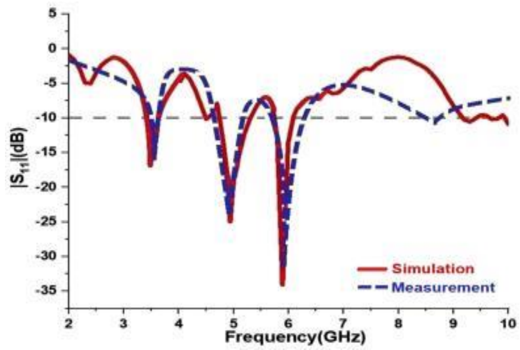

(a)

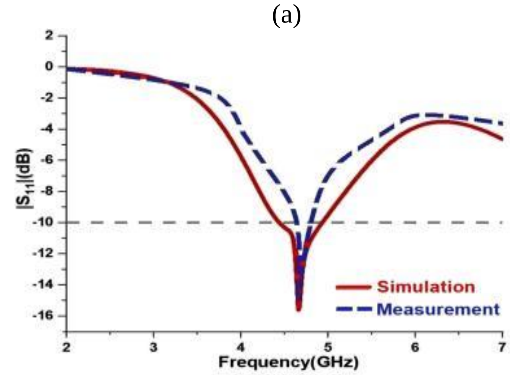

(b)

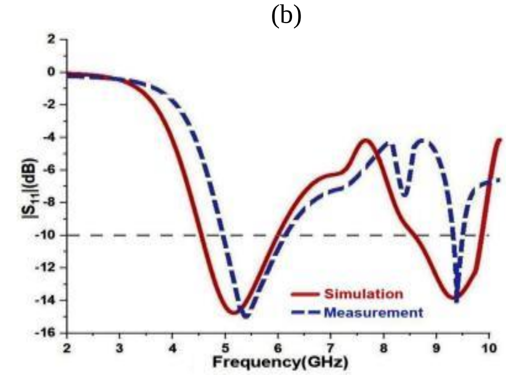

(c)

Fig. 8. Simulated and measured reflection coefficient of: (a) CP jute antenna, (b) cotton textile fabricated model, and (c) silk textile fabricated model.

The ARs of the jute textenna in the boresight direction were gauged. As shown in Fig. 9. A decent agreement between measured and simulated results are observed. The resonating frequency band where the AR is <3 dB ranges from 3.090-3.994, 4.85-4.95, and 5.70-5.85 respectively; hence, the jute textenna is CP, and it covers the WiMAX, WLAN, and ISM bands.

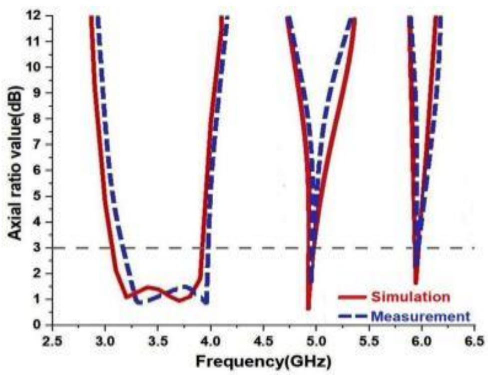

Fig. 9. Measured and simulated ARs of the CP jute textenna.

To demonstrate guaranteeing the CPn characteristic of the antenna. Figure 10 illustrates the +z surface current flow of the jute texteena at three operating frequencies, 3.5, 4.9, and 5.8 GHz. Likewise, in Fig. 10, relating to the changes of phase of the antenna, surface currents rotates in a round way in dextrorotatory direction. The explanation behind revolution can be named for two significant causes: (1) By utilizing asymmetric feed, it allows for flowing the currents in aside. Consequently, currents will move to the opposite side through the crescent path of the patch, and hence a CPn state occurs. (2) thus, that electrical charges consistently aggregate at keen points. In this way, the electrical charges on patch move to sharp end from the wide side end, for the most part, in keen end attached toward parasitic structure, and continually this procedure happens on the rear side of the substrate.

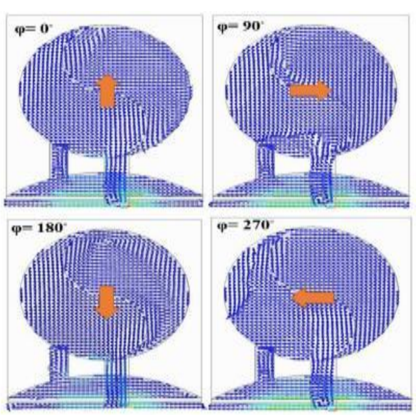

(a)

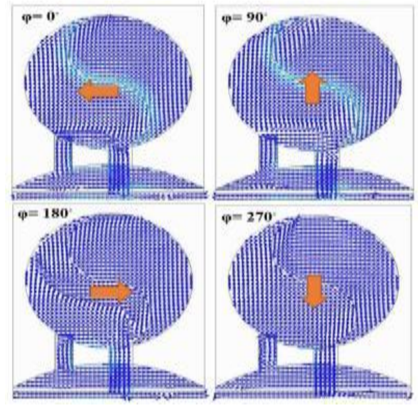

(b)

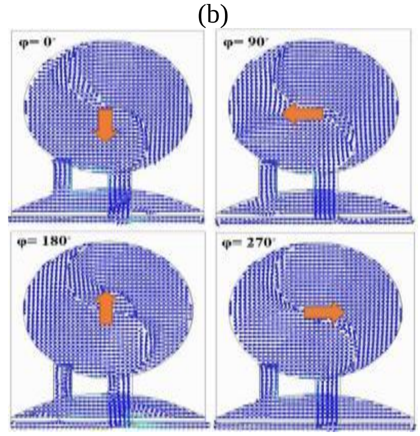

(c)

Fig. 10. Surface currents distribution of the jute textenna at +z for: (a) 3.5, (b) 4.9, and (c) 5.8 GHz.

The gain and efficiency characteristics of the proposed textenna are illustrated in Fig. 11, the gain values are 4.93, 8.86, 10.07 dBi at 3.5, 4.9, and 5.8 GHz (WiMAX, WLAN, ISM). Correspondingly the efficiency of the antenna in the resonating frequencies ranges from 83 to 89%.

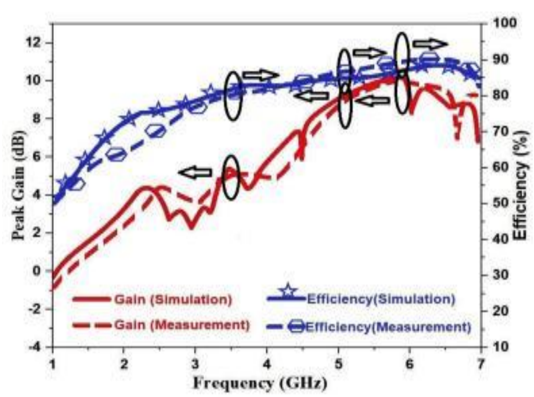

Fig. 11. Simulation and measured gain and efficiency of the proposed textenna.

IV. MEASUREMENT AND ANALYSIS

In addition to, the radiation characteristic of the CP jute textenna was validated in an anechoic chamber. The radiation patterns of LHCP and RHCP on the two principal planes (E-plane and H-plane) for 3.5, 4.9, and 5.8 GHz are as seen in Fig. 12.

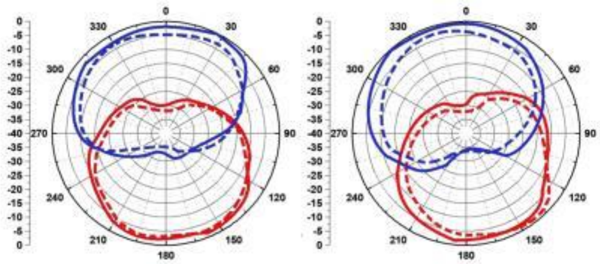

(a)

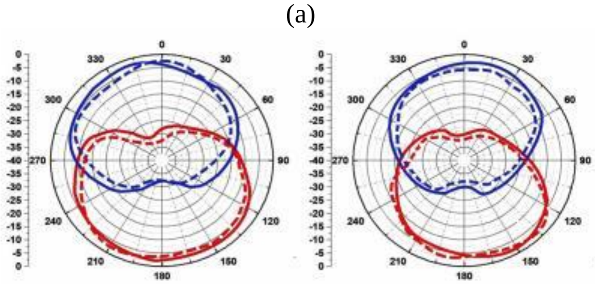

(b)

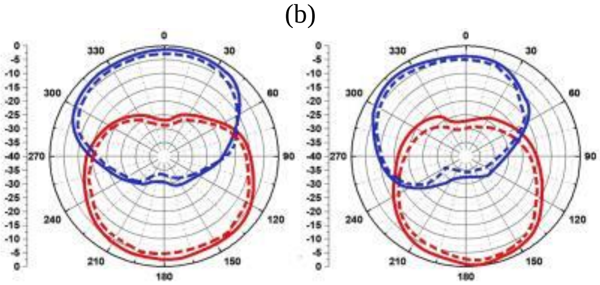

(c)

E-plane H-plane

Fig. 12. Measured and simulated radiation patterns at: (a) 3.5, (b) 4.9, and (c) 5.8 GHz. (Continuous blue line: RHCP simulated, dashed blue line: RHCP measured, continuous red line: LHCP simulated, dashed red line: LHCP measured).

Figure 13 shows the spectrum analyzer sensing results for different operating bands and the evidence of measurement.

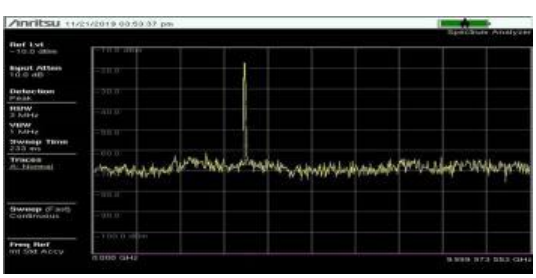

(a)

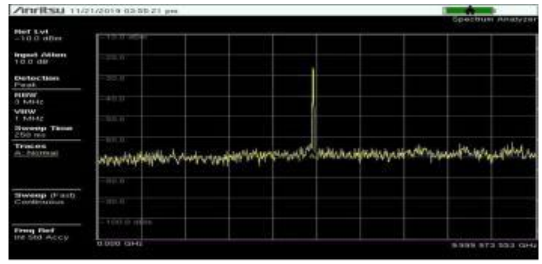

(b)

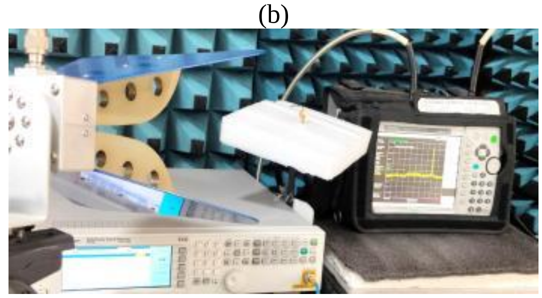

(c)

Fig. 13. Signal sensing and measurement setup: (a) 3.5, (b) 4.9 GHz, and (c) 5.8 GHz.

V. CONCLUSION

A circularly polarized jute textile substrate with a semicircular shaped antenna was proposed and actualized. The perfect demonstration of the antenna as far as radiation patterns, input matching, and axial ratios shows the high proficiency that can be acquired by espousing the jute material as the substrate. The textile antenna is distinguished by ease of fabrication, mechanical firmness, wide beamwidth, and a simple, semicircular based design. It creates the anticipated circular polarization for a strong radio frequency sensing link. Thus, the circularly polarized antenna paves the way for utilizing the components for exclusive exercises such as tracking and localization of rescue operations.

ACKNOWLEDGMENT

Authors want to thank the Department of Science and Technology, India, for supporting this work through the FIST Grant of SR/FST/ET-II/2019/450, and SEED/TIDE/2018/33/G.

REFERENCES

[1] A. G. Al-Sehemi, A. A. Al-Ghamdi, N. T. Dishovsky, N. T. Atanasov, and G. L. Atanasova, “Wearable antennas for body-centric communi-cations: Design and characterization aspects,” *Applied Computational Electromagnetics Society Journal*, vol. 34, no. 8, pp. 1172-1181, 2019.

[2] Y. Jiang, L. Xu, K. Pan, T. Leng, Y. Li, L. Danoon, and Z. Hu, “e-Textile embroidered wearable near-field communication RFID antennas,” *IET Microwaves, Antennas & Propagation*, vol. 13, no. 1, pp. 99-104, 2018.

[3] W. Huang and A. A. Kishk, "Compact antenna designs for wearable and portable medical system," *Applied Computational Electromagnetics Society Journal*, vol. 26, no. 4, pp. 295-302, 2011.
[4] X. Hu, S. Yan, and G. A. Vandenbosch, "Compact circularly polarized wearable button antenna with broadside pattern for U-NII worldwide band applications," *IEEE Transactions on Antennas and Propagation*, vol. 67, no. 2, pp. 1341-1345, 2018.
[5] Y. F. Lin, Y. C. Kao, S. C. Pan, and H. M. Chen, "Bidirectional radiated circularly polarized annular-ring slot antenna for portable RFID reader," *Applied Computational Electromagnetics Society Journal*, vol. 25, no. 3, pp. 182-189, 2010.
[6] M. L. Sabran, S. K. A. Rahim, P. J. Soh, C. Y. Leow, and G. Vandenbosch, "A simple electromagnetically fed circularly-polarized circular microstrip antenna," *Applied Computational Electromagnetics Society Journal*, vol. 30, no. 11, pp. 1180-1187, 2015.
[7] M. Tecpoyotl-Torres and J. G. Vera-Dimas, "Simulation, fabrication, and performance comparison of a GPS antenna with radome on the roof of an automobile," *Applied Computational Electromagnetics Society Journal*, vol. 28, no. 7, pp. 581-590, 2013.
[8] K. L. Chung, X. Yan, Y. Li, and Y. Li, "A Jia-shaped artistic patch antenna for dual-band circular polarization," *AEU- International Journal of Electronics and Communications*, vol. 120, 2020. doi.org/10.1016/j.aeue.2020.153207.
[9] J. Li, J. Shi, L. Li, T. A. Khan, J. Chen, Y. Li, and A. Zhang, "Dual-band annular slot antenna loaded by reactive components for dual-sense circular polarization with flexible frequency ratio," *IEEE Access*, vol 6, pp. 64063-64070, 2018.
[10] Y. Li and R. Mittra, "A three-dimensional circularly polarized antenna with a low profile and a wide 3-dB beamwidth," *Journal of Electromagnetic Waves and Applications*, vol. 30, no. 1, pp. 89-97, 2016.
[11] V. Zarei, H. Boudaghi, M. Nouri, and S. A. Aghdam, "Reconfigurable circular polarization antenna with utilizing active devices for communication systems," *Applied Computational Electromagnetics Society Journal*, vol. 30, no. 9, pp. 990-995, 2015.
[12] A. Sedghara and Z. Atlasbaf, "A new dual-band, dual-polarized, and single feed reconfigurable antenna," *Applied Computational Electromagnetic Society Journal*, vol. 31, no. 1, pp. 26-31, 2016.
[13] A. Alemaryeen and S. Noghanian, "AMC integrated textile monopole antenna for wearable applications," *Applied Computational Electromagnetic Society Journal*, vol. 31, no. 6, pp. 612-618, 2016.
[14] P. M. Paul, K. Kandasamy, and M. S. Sharawia, "Tri-band circularly polarized strip and SRR loaded slot antenna," *IEEE Transactions on Antennas and Propagation*, vol. 66, no. 10, pp. 5569-5573, 2018.
[15] Y. Hong, J. Tak, and J. Choi, "An all textile SIW cavity-backed circular ring slot antenna for WBAN applications," *IEEE Antennas and Wireless Propagation Letters*, vol. 15, pp. 1995-1999, 2016.
[16] S. Yan, V. Volskiy, and G. A. Vandenbosch, "Compact dual-band textile PIFA for 433-MHz/ 2.4-GHz ISM bands," *IEEE Antennas and Wireless Propagation Letters*, vol. 16, pp. 2436-2439, 2017.
[17] C. A. Balanis, *Antenna Theory: Analysis and Design*. John Wiley & Sons, New York, 2016.

Ram Sandeep Duvvada received his Bachelor and Master of Technology degrees from JNTUK in 2014 and 2017, respectively. Currently, he is pursuing Ph.D. in KLEF, Guntur, India. His research interests include flexible textile antennas and medical antennas.

N. Prabakaran received his Ph.D. degree from Satyabama University, India. Currently, he is working as an Associate Professor in the Department of ECE, KLEF. His research interests are wireless communications and wireless networks.

B. T. P. Madhav is working as Professor in ECE and Associate Dean at KLEF. He has published more than 292 papers in Scopus and SCI journals. He is a reviewer for several international journals including IEEE, Elsevier, Springer, Wiley, and Taylor and Francis.

K. L. Narayana is working as Professor & Dean (R&D) in the Department of ME at KLEF. He has around 40 + publications, out of which 29 are SCOPUS & WoS Journals. He is a life member of IME, CMSI, and ISTE. His research interests include materials, design and additive manufacturing of metals.